ISSN 2411-3336; e-ISSN 2541-9404

JOURNAL OF MINING INSTITUTE

Zapiski Gornogo instituta

Journal homepage: pmi.spmi.ru

Research article

Geotechnical Engineering and Engineering Geology

Investigation of the mass explosions impact on the off-contour massif

Evgenii B. Shevkun, Evgenii A. Shishkin✉
Pacific National University, Khabarovsk, Russia

How to cite this article: Shevkun E.B., Shishkin E.A. Investigation of the mass explosions impact on the off-contour massif. Journal of Mining Institute. 2026. Vol. 279, p. 13-24.

Abstract

The stress wave generated by rock blasting causes vibrations in the off-contour massif. The rock strength is significantly reduced in those off-contour massif areas where the permissible velocity is exceeded. This can lead to the collapse of nearby ledges. The aims of the study are to develop a methodology for determining the boundary of the off-contour massif seismically hazardous zone, as well as to assess the well delay interval effect on the hazardous zone boundary position. Elastic vibrations of the off-contour rock under the effect of a blast wave are considered. The dependence of the rock mass displacement under the action of stress is a function of time and distance from the blast site. A series of production experiments were conducted at the "Valley" quarry of Amur Minerals JSC to determine the coefficients values that take into account the attenuation of the stress wave in the rock with increasing distance from the blast site. A method to determine the position of the off-contour massif boundary has been developed. Beyond that boundary the rate of rock displacement does not exceed the permissible value. The initial data for the calculation are the rock mass physical and mechanical characteristics and the parameters of the explosives used. In the Simulink environment a simulation model was developed to implement the described method. A methodology for energy assessment of the process of rock displacement under the effect of a stress wave was developed to verify the modeling results. By analyzing the results obtained, a conclusion was made about the sufficient accuracy of the proposed method for practical calculations. Displacement energy values of the same point of the off-contour massif are compared at different well delay interval. Rock blasting with increased well delay intervals allows to improve the off-contour massif safety, as well as the overlying horizons ledges. The quality of blasted rock loosening is maintained.

Keywords

mass blast; elastic zone; wave of tension; displacement velocity; ledge; stability; well delay

Funding

The research was carried out at the expense of a grant from the Russian Science Foundation N 24-27-20036, https://rscf.ru/project/24-27-20036, and funding by Ministry of Education and Science of the Khabarovsk Region.

Received: 04.10.2025 ***Accepted: 24.12.2025*** ***Online: 14.05.2026***

Introduction

Blast loosening is an effective way to prepare rock for excavation [1-3]. The borehole charge blast causes a stress wave to occur. The amplitude values of the stress wave are less than rock tensile strength in the elastic zone of the off-contour massif [4, 5]. The stress wave causes elastic vibrations of the rock in this zone that can lead to destruction. The rock strength is significantly reduced when the permissible velocity is exceeded [6, 7]. Therefore, the speed of rock displacement is taken as an indicator for assessing the seismic effect of blast. Exceeding the velocity limit causes a significant decrease of the rock massif strength. It can lead to immediately collapse of nearby ledge [8, 9]. Off-contour zone elastic vibrations induce growth of microcracks in the nearby ledge [10, 11]. This can lead to "delayed fracture" due to subsequent impact of mining machinery (trucks, drilling rigs, etc.). Collapses at operating quarries (Kiembaevsky quarry, Vostochny quarry, etc.) confirm negative side of blast seismic action.

Of particular interest is the relation between peak value of the displacement velocity and distance from the blast site. In [12] an analytical dependence of the vibration velocity of massif on the distance between the outer row of wells of the blasting block and the measurement point is presented. It takes into account the degree of rock fracturing. As it is difficult to determine the dependence coefficients values, the practical application will be problematic. In [4] a coefficient equal to the ratio of the longitudinal wave velocity in a rock sample to the longitudinal wave velocity in the rock massif is proposed as a criterion for massif disturbance. However, the method for determining the massif disturbance coefficient is quite time-consuming. It is difficult to apply methods for assessing the vibration velocity at various distances from the protected object to the blast site [13-15]. The reason lies in the difficulty of determining the values of empirical coefficients, which depend on the blasting conditions and the propagation of seismic vibration.

Various methods are used to reduce the blast seismic hazard. An example is the screening blasting technology, which involves the formation of a crack in the rock mass as a result of the blast of closely spaced well charges of reduced diameter [16-18]. There are also other technological solutions, for example, injection strengthening of the rocks of the ledge slope [19]. However, the use of the described technological solutions leads to increased time-consuming and higher costs of blasting operations.

Varying the parameters of blasting operation with the quality of rock crushing maintained is the preferred method of reducing the seismic impact of the blast on the off-contour massif. The best way to control the seismic action of the blast is by adjusting the delay time of the well charges [20-22]. The disturbance intensity of the off-contour massif can be reduced by assigning a delay time interval sufficient for the formation of a free surface [23]. Experimental studies in limestone quarries [24] have shown that well delay interval over 42 ms leads to a reduction in the maximum amplitude of the massif vibration velocity by up to 2.2 times. Theoretical studies [25] have shown that increasing the delay interval leads to a predominance of low frequencies in the oscillation spectrum. Therefore, the use of delay interval greater than 60 ms allows to increase the stability of the mine workings. However, existing studies have poorly studied the influence of delay intervals greater than 100 ms on the preservation of the off-contour massif.

The purpose of the study is to develop a relatively easy-to-use methodology for determining the seismically safe distance, as well as to experimentally confirm the positive effect of the well delay interval of over 100 ms on the value of the seismically safe distance.

Methodology

In the elastic deformation zone the rock massif is a linear-elastic medium with attenuation [26, 27]. Which means that rock behaves as a linear-elastic body at any point,

$$\sigma(t) = ku(t), \tag{1}$$

where σ stands for the stress, Pa; k stands for the proportionality coefficient characterizing the rigidity of a rock; u stands for the displacement, m.

As you move away from the excitation source, the signal weakens (attenuates) due to energy dissipation [28]

$$\sigma_{max} = \sigma_{max}(r), \tag{2}$$

where σ_{max} stands for the maximum stress reached at the point in question, Pa; r stands for the distance from the excitation source to the point in question, m.

Thus, at any medium point, the excitation wave stress is a function of time t and distance r from the excitation source, $\sigma = f(t, r)$.

The ascending branch of the positive phase of the function $\sigma(t)$ can be described using a parabolic function

$$\sigma(t) = -ct^2 + 2\sqrt{cdt}, \quad (3)$$

where c stands for the coefficient depending on the time t_{max} of reaching the maximum value σ; $\sigma = \sigma_{max}$; d stands for the coefficient depending on the pulse amplitude σ_{max}.

After substituting in (1) the equation (3) we obtain the displacement $u(t)$ for a specific point of the massif

$$u(t) = -\frac{c}{k}t^2 + \frac{2}{k}\sqrt{cdt}, \quad (4)$$

let's transform the equality (4)

$$u(t) = -at^2 + 2\sqrt{abt}, \quad (5)$$

where a stands for the coefficient depending on the time t_{max} of reaching the maximum value $u = u_{max}$; b stands for the coefficient depending on the displacement amplitude u_{max}.

From equation (5) it follows that the displacement function $u(t)$ repeats the function of the exciting pulse $\sigma(t)$, but with different coefficients:

$$a = \frac{u_{max}}{t_{max}^2}; \quad b = u_{max}. \quad (6)$$

The displacement u described by equation (5) is a function of time t and distance r from the excitation source $u = f(t, r)$. At a distance r from the explosion site, the attenuation of the stress wave in the rock is taken into account by the coefficients a, b: $a = f(r)$; $b = f(r)$. In the "Valley" quarry of Amur Minerals JSC (Khabarovsk Region) a series of production experiments were carried out to obtain values of time t_{max} and the corresponding displacement u_{max} used in equation (6).

The experimental conditions are as follows:

• explored horizons – 180-170, 170-165, 150-140;

• the rocks are represented by quartz-feldspar sandstone, potassium-feldspar compositions from light gray to gray in color with bundles of biotite;

• well delay – 42×67 ms, 176×200 ms;

• tamping type – drilling fines;

• the initiation of the distribution network was carried out by the non-electrical Iskra system (Russia);

• physical and mechanical properties of rock (Protodyakonov strength index f = 11-13; density ρ_0 = 2650 kg/m^3; compressive strength σ_{compr} = 92 MPa; tensile strength σ_{tens} = 7.2 MPa; Young's modulus E = 27.8 GPa; Poisson's ratio ν = 0.27).

Geophones were installed at a distance of 20 m from the block boundary (Fig.1). The measurements were carried out using the Laccolith 24-M2 seismic survey station recording complex. (Russia) (Fig.2, *a*). The ADC resolution of the complex is 24 bits. Geophones GS-20DX (USA) were connected to the seismic streamer of the recording complex (Fig.2, *b*); geophone sensitivity $\alpha = 27.6 \times \times 10^3$ μV/(mm/s).

The seismoacoustic source generated an excitation pulse. Geophones (Fig.2, *b*) recorded the pulse at different distances from the excitation point. The geophone signals were converted by the recording complex (Fig.2, *a*) into discrete U values, displayed on the laptop screen in the form of a seismic trace.

Journal of Mining Institute. 2026. Vol. 279. P. 13-24

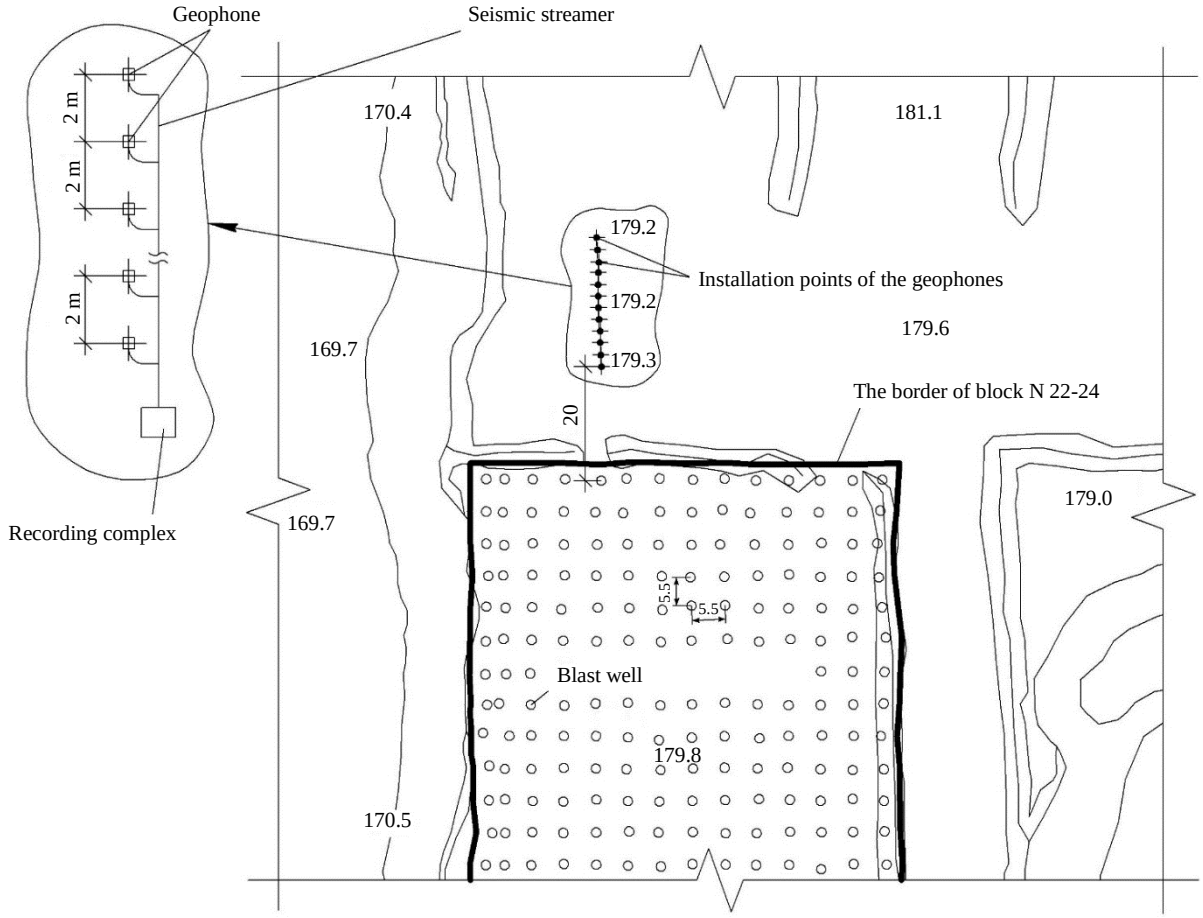

Fig.1. The layout of the geophones relative to block N 22-24

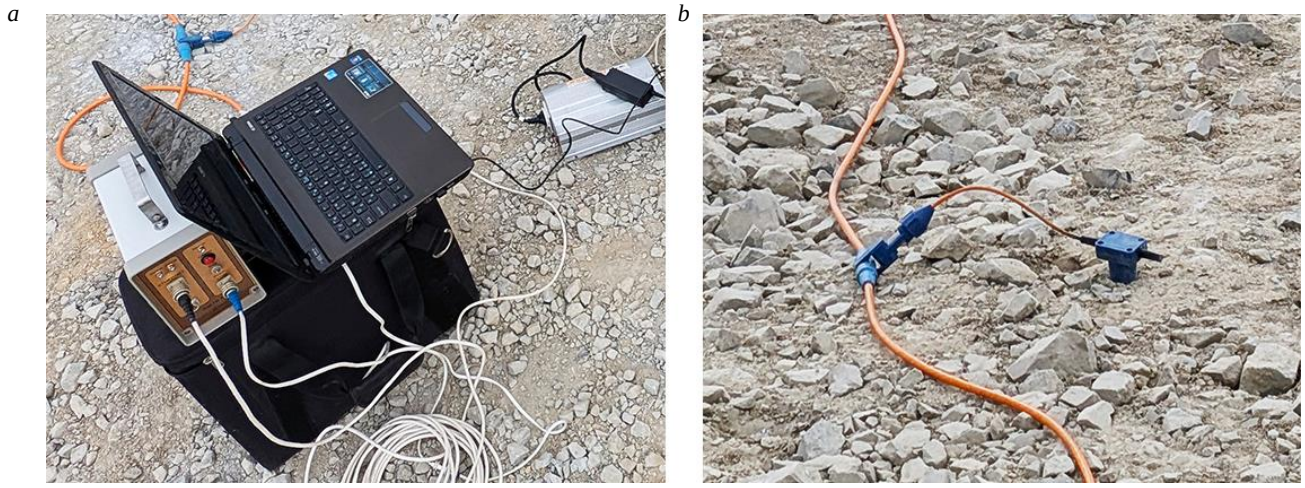

Fig.2. Laccolith 24-M2 seismic survey station: *a* – recording complex; *b* – geophone

The transformation of *U* values into the value of the rock displacement velocity was carried out according to the dependence

$$\dot{u} = \frac{U}{\alpha}, \tag{7}$$

where α stands for the geophone sensitivity, μV/(mm/s).

The positive phase of the pilot pulse (Fig.3), recorded by the seismic survey station, can be described by the following dependence:

$$\dot{u}(t) = \dot{u}_{\max} \sin(\omega t), \quad (8)$$

where $\dot{u}$ stands for the rock displacement velocity, mm/s; $\dot{u}_{\max}$ stands for the maximum rock displacement velocity, mm/s; ω stands for the pulse frequency, rad/s.

The abscissa of the curve maximum $\dot{u}(t)$ is equal to $t'_{\max} = T/4$, where T stands for the period of oscillation (Fig.3); pulse frequency

$$\omega = \frac{\pi}{2t'_{\max}}. \quad (9)$$

We integrate (8) to obtain the dependence of rock displacement $u(t)$:

$$u(t) = \int \dot{u}_{\max} \sin(\omega t) dt. \quad (10)$$

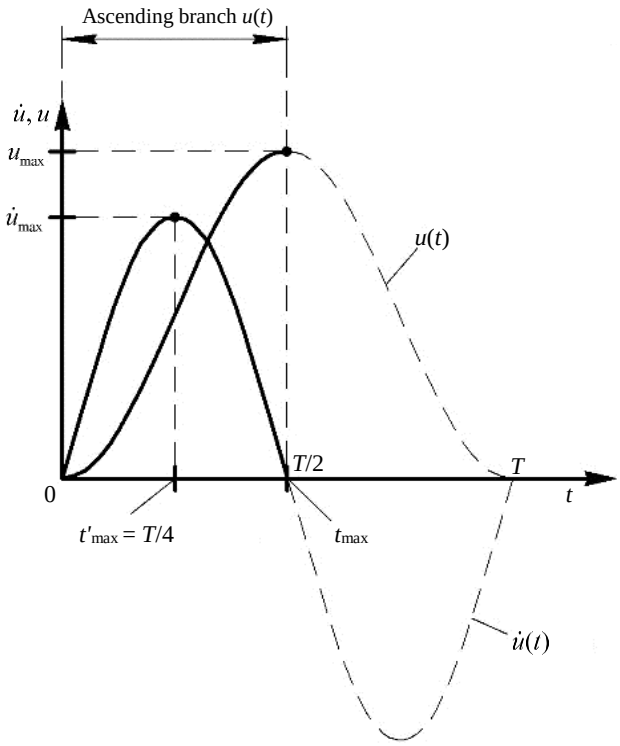

Fig.3. Time dependence of displacement and displacement velocity of rock

Taking into account the initial conditions $t = 0$, $u = 0$, we obtain (Fig.3)

$$u(t) = \frac{\dot{u}_{\max}}{\omega}\left[1 - \cos(\omega t)\right]. \quad (11)$$

The moment $t_{\max} = T/2$ is equal to

$$t_{\max} = \frac{\pi}{\omega} = 2t'_{\max}; \quad (12)$$

amplitude of displacement

$$u_{\max} = \frac{2\dot{u}_{\max}}{\omega}. \quad (13)$$

Taking into account (12), (13), equations (6) are:

$$a = \frac{\dot{u}_{\max}}{\pi t'_{\max}}; \quad b = \frac{4\dot{u}_{\max} t'_{\max}}{\pi}. \quad (14)$$

The a and b coefficients are calculated using equations (14) taking into account the values of $t'_{\max}$ and $\dot{u}_{\max}$ obtained for different distances r. The distance r is measured from the boundary between the elastic deformation zone and the crushing zone. The coefficients $a_0(r = 0)$ and $b_0(r = 0)$, calculated for the boundary of the elastic deformation zone and the crushing zone, were added to the arrays $a_i(r_i)$ and $b_i(r_i)$. After that, statistical processing of the data arrays was carried out. For physical reasons, an exponential dependence was chosen as the approximating function, since it describes the weakening of an elastic wave during its propagation in a dissipative medium [29]. During the approximation, the least squares method was used, the coefficient of determination R^2 was 0.88.

At the boundary of the elastic deformation zone and the crushing zone, i.e. at $r = 0$, according to equation (6),

$$a_0 = \frac{u_{\max 0}}{t_{\max 0}^2}; \quad b_0 = u_{\max 0}, \tag{15}$$

where $u_{\max 0}$ stands for the maximum displacement of rock at the boundary of the elastic deformation zone; $t_{\max 0}$ stands for the time to reach maximum displacement $u_{\max 0}$.

Maximum displacement, according to [30],

$$u_{\max 0} = \frac{1+\nu}{E}\sigma_{\text{tens}} R, \tag{16}$$

where ν stands for the Poisson's ratio of a rock; E stands for the Young's modulus of a rock, Pa; σ_{tens} stands for the tensile strength of rock, Pa; R stands for the distance from the blast site to the boundary of the elastic deformation zone, m.

Time to reach the maximum displacement [31]

$$t_{\max 0} = \frac{54}{K} R^{1-\frac{\nu}{2(1-\nu)}} Q^{0.05}, \tag{17}$$

where K stands for the volumetric modulus of elasticity of rock, Pa; Q stands for the blast charge mass, kg.

According to [30], the distance from the blast site to the boundary of the elastic deformation zone

$$R = \frac{\nu}{1+\nu}\frac{\sigma_{\text{compr}}}{\sigma_{\text{tens}}} r_0 \left[\frac{\rho_{\text{EM}} D^2}{8\sigma_{\text{compr}}\left(\frac{\rho_0 C_w^2}{\sigma_{\text{compr}}}\right)^{1/4}}\right]^{1/4} \left(\frac{\rho_0 C_w^2}{5\sigma_{\text{compr}}}\right)^{1/2}, \tag{18}$$

where σ_{compr} stands for the compressive strength of rock, Pa; r_0 stands for the charge radius, m; ρ_{EM} stands for the explosive material density, kg/m^3; ρ_0 stands for the rock density, kg/m^3; C_w stands for the longitudinal wave velocity, m/s; D stands for the detonation velocity of explosive material, m/s.

Substituting (16), (17) into equations (15), we obtain

$$a_0 = \frac{(1+\nu)\sigma_{\text{tens}} K^2 R^{\frac{\nu}{1-\nu}-1}}{2916 E Q^{0,1}}; \quad b_0 = \frac{1+\nu}{E}\sigma_{\text{tens}} R. \tag{19}$$

An approximation of the values $a_i(r_i)$ and $b_i(r_i)$, obtained on the basis of $\dot{u}_{\max}$, $t'_{\max}$ according to formulas (14), as well as the values of the coefficients a_0, b_0, calculated according to formulas (19), was performed. As a result, the following exponential dependencies were obtained:

$$a = m_1 e^{-n_1 r}; \quad b = m_2 e^{-n_2 r}, \tag{20}$$

where m_1, m_2, n_1, n_2 stands for the coefficients depending on the physical and mechanical characteristics of the rock, for quartz-feldspar sandstone $m_1 = 6.962 \cdot 10^{20}$, $m_2 = 8783$, $n_1 = 0.472$, $n_2 = 0.609$; r stands for the distance to the oscillation excitation source, m.

The seismically safe distance from the blast site is determined by comparing the maximum displacement velocity $\dot{u}_{\max}$ with the permissible $\dot{u}_{\text{p}}$:

• For the distance $r_0 = 0$ the values of a_0, b_0 are calculated according to the dependencies (19). We obtain the dependence $u_0(t)$ at the boundary of the elastic zone by substituting the values of the coefficients a_0, b_0 into equation (5). The value of the displacement velocity $\dot{u}_{\max 0}$ for the moment of

time $t = 0$ is determined by differentiating the obtained dependence. We compare the obtained speed value with the permissible speed $\dot{u}_p$. If $\dot{u}_{max0} > \dot{u}_p$, we increase the distance r_0 by Δr. The result is $r_1 = r_0 + \Delta r$.

• According to dependencies (20), the values a_1, b_1 are determined for the distance r_1. Substituting the values a_1, b_1 into equation (5), we obtain the dependence $u_1(t)$ for the distance r_1 from the boundary of the elastic zone. Once the obtained dependence is differentiated, we determine the value of the displacement velocity $\dot{u}_{max1}$ for the moment of time $t = 0$. We compare the obtained speed value with the permissible speed $\dot{u}_p$. If $\dot{u}_{max1} > \dot{u}_p$, we increase the distance r_1 by Δr. The result is $r_2 = r_1 + \Delta r$.

The algorithm is repeated until the condition $\dot{u}_{max} \le \dot{u}_p$ is met. In this case, the distance $(r_n + R)$ is taken as acceptable, since the distance r is measured from the boundary of the elastic deformation zone.

According to [32], for sandstone characterized by a compressive strength of 92 MPa, a tensile strength of 7.2 MPa, and a Young's modulus of 27.8 GPa, the permissible value of the displacement velocity of the rock $\dot{u}_p$ is 14 cm/s.

The value of the longitudinal wave velocity C_w for (18) was determined based on the results of measurements from the seismic exploration station. The time of the first arrival of a longitudinal wave [33, 34], reaching the geophone i was recorded on the seismic trace. This time corresponds to the first deviation of the medium particles from the zero position. The signal propagation velocity from the source of seismic acoustic vibrations to the geophone i was determined by the dependence

$$C_i = \frac{\Delta u_{gi}}{\Delta t_{gi}}, \tag{21}$$

where Δu_{gi} stands for the distance from the source of seismic acoustic vibrations to geophone i, m; Δt_{gi} stands for the signal travel time from the source of seismic acoustic vibrations to geophone i, s.

The average longitudinal wave velocity C_w was calculated based on the longitudinal wave velocity values of the geophones C_i.

Figure 4 shows the structural diagram of the simulation model for determining the seismic safety distance. The model includes the following subsystems: 1 – initial data; 2 – determination of the coefficients a_0 and b_0 at the boundary of the elastic deformation zone; 3 – approximation – obtaining exponential dependencies (20); 4 – determination of the maximum velocity of rock displacement at a distance r_i from the blast site; 5 – condition for iterations end – $\dot{u}_{max} \le \dot{u}_p$; 6 – modeling result – the value of the seismically safe distance, m.

An energy assessment of the process of rock displacement under the action of a stress wave was carried out to confirm the proposed method.

Let $u(t)$ be a function of rock displacement under stress $\sigma(t)$. Let us consider the displacement u of the rock from the initial position to the position of maximum displacement over time t_{max}, i.e. the ascending branch of the function $u(t)$ (Fig.3). Displacement work

$$A = Fu, \tag{22}$$

where F stands for the radial force acting on rock; u stands for the rock displacement.

Let us select a unit area in the rock that is perpendicular to the stress σ. Then the force F applied to this area will be equal to the stress σ. The energy required to move this area

$$Э = \int_0^{t_{max}} \sigma(t) u(t) dt. \tag{23}$$

Law (1) is valid for maximum values of stress in the rock and displacement of the rock at the boundary of the elastic deformation zone, since the rock is considered as a linear-elastic body

Journal of Mining Institute. 2026. Vol. 279. P. 13-24

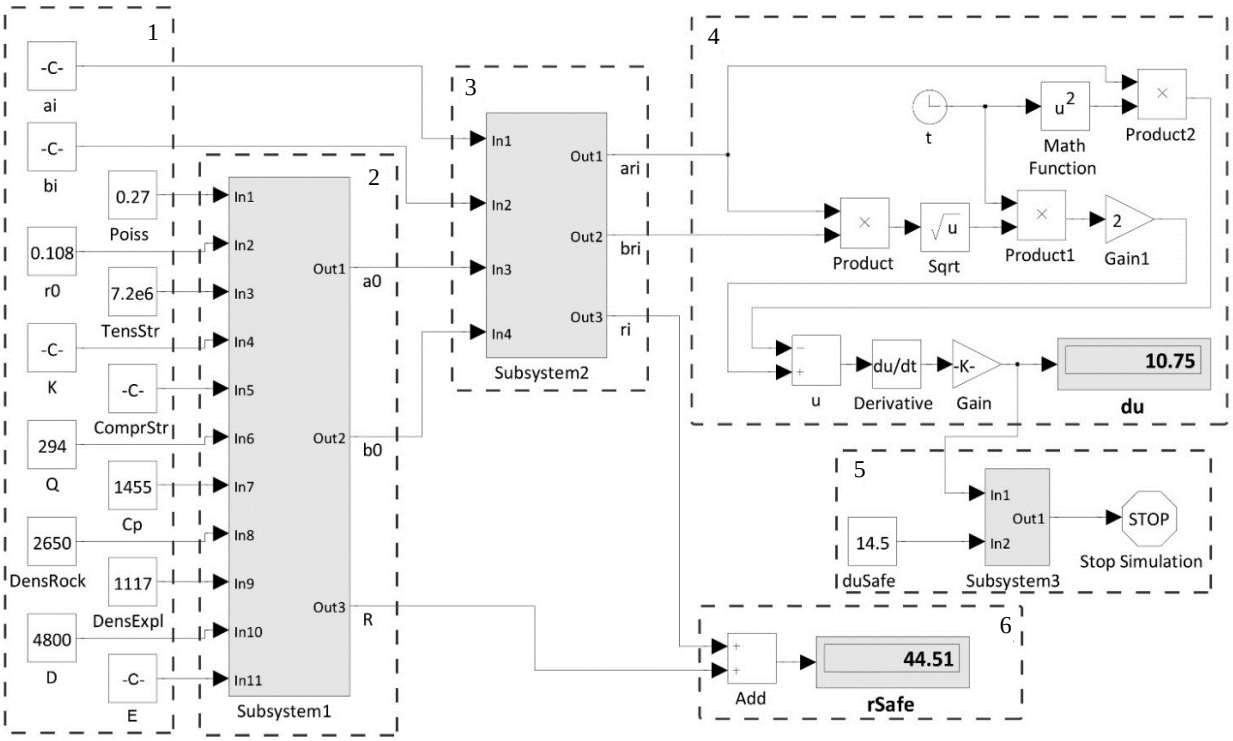

Fig.4. Simulation model diagram in the Simulink environment

$$\sigma_{\max 0} = k u_{\max 0}, \tag{24}$$

where σ_{max0} stands for the maximum stress at the boundary of the elastic deformation zone.

From (24) we obtain the coefficient of rock rigidity,

$$k = \frac{\sigma_{\max 0}}{u_{\max 0}}. \tag{25}$$

According to [30], the amplitude value of stress at the boundary of the elastic deformation zone

$$\sigma_{\max 0} = \sigma_{\text{tens}}. \tag{26}$$

Taking into account (16), (24), (25), (26), equation (23) takes the form:

$$W = \frac{E}{(1+\nu)R} \int_0^{t_{\max}} u^2(t)\, dt. \tag{27}$$

Only the ascending branch of the signal $u(t)$ is considered, i.e., for $t > t_{max}$, the function values are assumed to be zero. Therefore, the upper limit of integration (27) can be changed to ∞:

$$W = \frac{E}{(1+\nu)R} \int_0^{\infty} u^2(t)\, dt. \tag{28}$$

The Rayleigh theorem, known from spectral analysis, has the form

$$\int_0^{\infty} f^2(t)\, dt = \frac{1}{\pi} \int_0^{\infty} F^2(\omega)\, d\omega, \tag{29}$$

where $f(t)$ stands for some function; $F(\omega)$ stands for the spectral density of a function $f(t)$; ω stands for the frequency.

Comparing equations (28) and (29) and choosing the function $f(t)$ as $u(t)$, we have the equation

$$W = \frac{E}{(1+\nu)R}\int_0^\infty u^2(t)\,dt = \frac{E}{\pi(1+\nu)R}\int_0^\infty F^2(\omega)\,d\omega. \quad (30)$$

The area enclosed by the spectrum of the displacement function $u(t)$ squared, multiplied by the coefficient $E/\pi(1 + \nu)R$, is equal to the energy required to displace the rock within a unit area according to the law $u(t)$.

The measuring equipment was used to obtain energy values at different distances from the blast site and well delays. The marking of the installation points of the seismic receivers was carried out using a Topcon Hiper VR UHF/GSM receiver in a set with an FC-500 field controller, installed on a portable pole. The measured coordinates of the points were entered into the controller's memory with reference to the terrain plan within the boundaries of the block to blast. This procedure was carried out to find locations for geophone installations after a mass blast of the block in order to conduct repeated measurements.

The values of medium point displacement velocity obtained with the help of Laccolith 24-M2 give the displacements after integration. The amplitude spectrum $F(\omega)$ of the displacement signal $u(t)$ up to the moment t_{max} was obtained using the fast Fourier transform algorithm. The power spectrum $F^2(\omega)$ is obtained by squaring the values of the amplitude spectrum $F(\omega)$ (Fig.5). The spectrum contains uncharacteristic high-frequency components. This is due to the spectral decomposition of just a portion of the displacement signal $u(t)$ with a duration of t_{max}. As is known from spectral analysis, a shorter signal has a wider spectrum. In addition, the spectral displacement signal exhibits a sharp decline at time $t = t_{max}$ (see Fig.3). This also adds high-frequency components to the spectrum.

The area under the curve on the power spectrum graph corresponds to the value of $\int_0^\infty F^2(\omega)\,d\omega$. Let's substitute this value into equation (30). As a result, we obtain the numerical value of the energy required to displace the rock under the action of a stress pulse $\sigma(t)$. This value can serve as an indirect measure of the massif disturbance as a blast result.

The difference in energy values before and after the rock blast is calculated using equation

$$\Delta W = 100\,\% - \frac{W_2}{W_1}\cdot 100\,\%, \quad (31)$$

where W_1 stands for the energy for displacement of rock before blast; W_2 stands for the energy for displacement of rock after blast.

Discussion

Modeling (Fig.4) of the blast impact on the off-contour massif consisting of quartz-feldspar sandstone was performed. The resulting seismic safety distance was 44.51 m. The estimated value of rock displacement is less than the permissible value: $\dot{u}_{max}$ = 10.75 sm/s < $\dot{u}_p$ = 14 sm/s.

Energy values were calculated for massif points located at different distances from the blast site. The result was that at a distance of 26 m from the blast site, ΔW = 36.4 % (Fig.5, *a*), and at a distance of 45 m, ΔW = 5.8 % (Fig.5, *b*). Therefore, there is no seismic impact at a distance of more than 45 m from the blast site. This distance is seismically safe.

In all measurement series, the discrepancy between the calculated and experimental values of the safe distance did not exceed 7 %. That is, the developed simulation model is adequate.

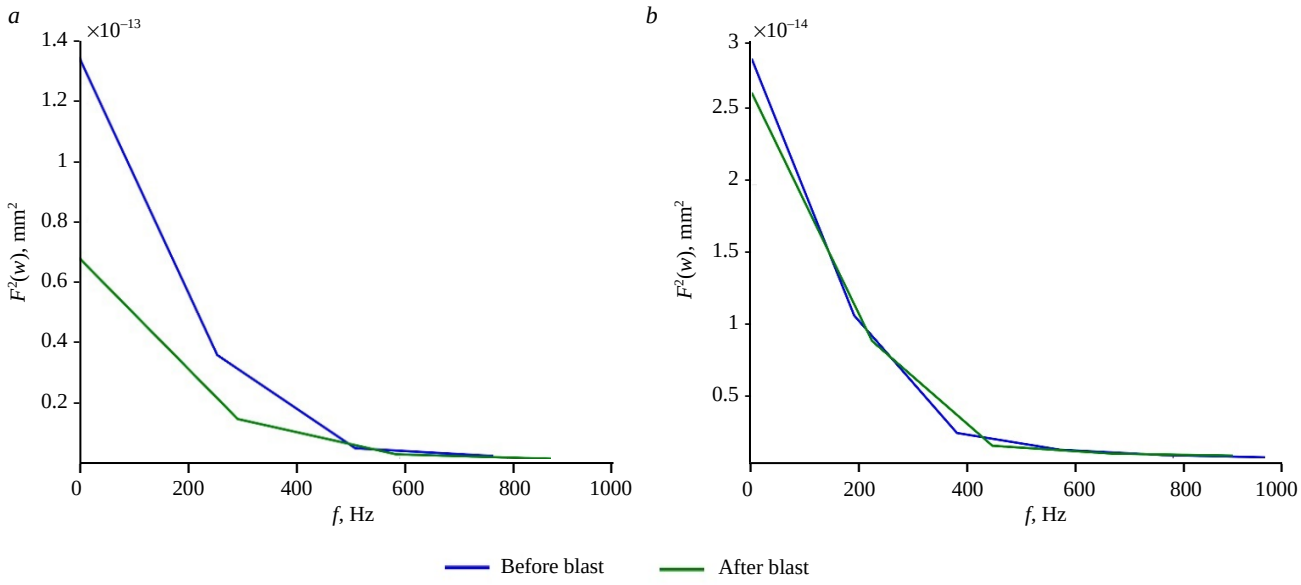

Fig.5. Signal power spectrum $u(t)$ for points located at distances: *a* – 26 m; *b* – 45 m from the blast site

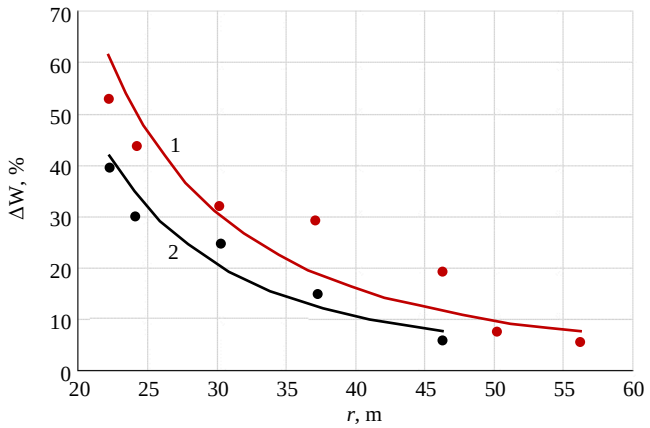

Fig.6. The influence of well delay time
on stress wave attenuation:
1 – delay time in a row is 42 ms, between rows – 67 ms;
2 – delay time in a row is 176 ms, between rows – 200 ms

Calculations of the energy value W for rock displacement were made to assess the influence of well delay on the seismic safety distance. The positive effect of increased delay on the seismically safe distance value was identified by comparing the energy discrepancies ΔW for different delays (Fig.6).

Increasing the delay up to 200 ms allows to reduce the seismic impact on the off-contour massif. Increasing the delay interval ensured the completion of the cracking process in the charge's impact zone. Most of the blast energy was expended on fragmentation, thereby reducing the seismic impact. When blasting with a delay of 176×200 ms, ΔW_2 is on average 1.83 times less than ΔW_1 when blasting with a delay of 42×67 ms. Seismic safety distance decreased when blasting with an increased delay: 176×200 ms gives 46 m; 42×67 ms gives 56 m.

Conclusion

The developed method for assessing rock displacement velocity allows for the determination of seismic safety distances with sufficient accuracy for practical calculations. The initial data are the physical and mechanical properties of the rock and the blasting process parameters. The developed method for determining the energy of rock displacement allows for indirect assessment of the off-contour massif disturbance under the action of a blast wave. It was found that increasing the delay between rows of well charges from 67 to 200 ms makes it possible to reduce the seismically safe distance by 1.2 times (from 56 to 46 m for sandstone). Thus, rock mass blasting with an increased delay improve off-contour massif safety, including ledges of the overlying horizons.

The great advantage of the developed method for determining seismically safe distance is its relative simplicity. To implement the method, only a seismic survey station is required. The method does not require laboratory testing. Using the developed method will improve both the current stability of ledges and the stability of ledges at the quarry's boundary.

The authors express their gratitude to Amur Minerals JSC (*Khabarovsk Region*) *for the opportunity to conduct an instrumental assessment of changes in the parameters of rock mass disturbance near blasted industrial blocks under various parameters of mass blasts*.

REFERENCES

1. Shevkun E.B., Plotnikov A.Yu., Nikulin P.V., Kazarina E.N. Loosing of rocks by blasting without disintegration at open pit mines. *Gornyi zhurnal.* 2024. N 6, p. 76-81 (in Russian). DOI: 10.17580/gzh.2024.06.12

2. Pytalev I.A., Domozhirov D.V., Ugolnikov N.V. et al. Ensuring high quality of explosive preparation of rocks for excavation with open method of mining under difficult mining and geological conditions and significant growth of the scope of work. *Mine Surveying Bulletin.* 2021. N 5-6 (144-145), p. 116-121 (in Russian).

3. Afanasyev P.I., Menzhulin M.G. Change in the average lump size in the crushing zone based on the calculation of energy dissipation. *News of the Tula State University. Sciences of Earth.* 2022. N 4, p. 408-419 (in Russian).

4. Kovalchuk I.O., Kondrashov A.V., Dobrynin A.A. Rock mass disturbance clarification close to blast block through P-wave measuring. *Transactions of RANIMI.* 2024. N 2 (40), p. 101-105 (in Russian). DOI: 10.24412/2519-2418-2024-240-101-105

5. Gospodarikov A.P., Revin I.E., Morozov K.V. Composite model of seismic monitoring data analysis during mining operations on the example of the Kukisvumchorrskoye deposit of AO Apatit. *Journal of Mining Institute.* 2023. Vol. 262, p. 571-580. DOI: 10.31897/PMI.2023.9

6. Tyupin V.N. Geometric parameters of the seismic focus zone during mass explosions in quarries. *Explosion Technology.* 2022. N 134/91, p. 137-154 (in Russian).

7. Yakovlev A.V., Shimkiv E.S. Problems of ultimate pit limit design. *Mining Informational and Analytical Bulletin.* 2021. N 5-1, p. 105-116 (in Russian). DOI: 10.25018/0236_1493_2021_51_0_105

8. Xueliang Zhu, Shuai Shao, Shengjun Shao et al. A general kinematic approach to the effect of rock mass saturation on the stability of 3D rock slopes. *Environmental Earth Sciences*. 2025. Vol. 84. Iss. 1. N 9. DOI: 10.1007/s12665-024-11992-6

9. Belov A.A., Afanasev P.I., Shmonin I.V. Development of a comprehensive analysis of seismic blast impact on the quarry marginal massif: theoretical approaches, methodologies and challenges. *Explosion Technology.* 2025. N 146/103, p. 102-132 (in Russian). DOI: 10.18698/0372-7009-2023-9

10. Romanenko S.V., Larionova E.V., Muldybaev U.A. et al. Risk management technique of landslides activation with account of seismic activity factor in Kyrgyzstan. *Bulletin of the Tomsk Polytechnic University. Geo Assets Engineering.* 2020. Vol. 331. N 10, p. 155-163 (in Russian). DOI: 10.18799/24131830/2020/10/2865

11. Xiaohua Ding, Yuqing Yang, Wei Zhou et al. The law of blast stress wave propagation and fracture development in soft and hard composite rock. *Scientific Reports.* 2022. Vol. 12. N 17120. DOI: 10.1038/s41598-022-22109-z

12. Tyupin V.N. Seismic effects induced by large-scale blasts in isotropic and structurally complex pit wall rock masses. *Mining Informational and Analytical Bulletin.* 2021. N 12, p. 47-57 (in Russian). DOI: 10.25018/0236_1493_2021_12_0_47

13. Singh P., Jayanthu S. Pseudo-static and Dynamic Analysis of Mine Rock Slope Under the Influence of Production Blasting. *Mining, Metallurgy & Exploration*. 2024. Vol. 41. Iss. 6, p. 3197-3209. DOI: 10.1007/s42461-024-01112-0

14. Hengyu Su, Shu Ma. Study on the stability of high and steep slopes under deep bench blasting vibration in open-pit mines. *Frontiers in Earth Science*. 2022. Vol. 10. N 990012. DOI: 10.3389/feart.2022.990012

15. Tingyao Wu, Chuanbo Zhou, Nan Jiang et al. Stability analysis for high-steep slope subjected to repeated blasting vibration. *Arabian Journal of Geosciences*. 2020. Vol. 13. Iss. 17. N 828. DOI: 10.1007/s12517-020-05857-y

16. Kantor V.Kh., Rakhmanov R.A., Alenichev I.A. et al. Investigation of the parameters of contour borehole explosive charges for the formation of a cut-off gap in rocks during the cutting of ledges in quarries. *Explosion Technology.* 2022. N 135/92, p. 32-66 (in Russian).

17. Kamyansky V.N. Estimation of seismic load of blasting on pit wall rock mass during blasted slot making. *Mining Informational and Analytical Bulletin.* 2018. N 7, p. 181-188 (in Russian). DOI: 10.25018/0236-1493-2018-7-0-181-188

18. Shemetov P.A., Umarov F.Ya. Seismically safe method of drilling-and-blasting in pitwall rocks and at engineering structures. *Mining Informational and Analytical Bulletin.* 2013. N 8, p. 221-224 (in Russian).

19. Uglyanitsa A.V. Deep injection benchmarks for increasing the stability of open pit walls. *Bulletin of the Kuzbass State Technical University.* 2023. N 1 (155), p. 87-94 (in Russian). DOI: 10.26730/1999-4125-2023-1-87-94

20. Shevkun E.B., Leshchinskiy A.V., Lysak Yu.A., Plotnikov A.Yu. Long-period delay loosening blasting in open pit mines. *Mining Informational and Analytical Bulletin.* 2020. Vol. 10, p. 29-41 (in Russian). DOI: 10.25018/0236-1493-2020-10-0-29-41

21. Peng Xu, Renshu Yang, Jinjing Zuo et al. Research progress of the fundamental theory and technology of rock blasting. *International Journal of Minerals, Metallurgy and Materials*. 2022. Vol. 29. Iss. 4, p. 705-716. DOI: 10.1007/s12613-022-2464-x

22. Lyashenko V.I., Kislyy P.A. Justification seismic safety technologies destruction massif slozhnostruktural fields. *Mining Informational and Analytical Bulletin.* 2017. N 6, p. 314-332 (in Russian).

23. Yakovlev A.V., Shimkiv E.S., Perekhod T.M. The main directions and results of research of crushing of hard-to-blast rocks. *Problems of Subsoil Use.* 2019. N 3 (22), p. 137-144 (in Russian). DOI: 10.25635/2313-1586.2019.03.137

24. Bulbasheva I.A. Management of blasts seismic effect on transmission line supports during open-pit mining: Avtoref. dis. … kand. tekhn. nauk. St. Peterburg: Sankt-Peterburgskii gornyi universitet, 2019, p. 19 (in Russian).

25. Zykov V.S., Ivanov V.V., Sobolev V.V. Studies of the Effect of Massive Industrial Explosions on the Stability of the Underground Mining Workings at the Open-pit and Underground Mining of Coal Deposits. *Occupational Safety in Industry.* 2018. N 11, p. 19-23 (in Russian). DOI: 10.24000/0409-2961-2018-11-19-23

26. Kozyrev S.A., Vlasova E.A., Usashev E.A. Engineering methodology for operative assessment of seismic blast impact in the boundary rock mass in open pits. *Russian Mining Industry.* 2024. N 5, p. 66-73 (in Russian). DOI: 10.30686/1609-9192-2024-5-66-73

27. Li Chengjie, Wang Mengqi, Xie Shoudong et al. Experimental investigation of blasting stress wave attenuation in sandstone with columnar charging using high-speed DIC technique. *Scientific Reports*. 2025. Vol. 15. N 22515. DOI: 10.1038/s41598-025-02662-z

28. Shuailong Jia, Zhiliang Wang, Jianguo Wang et al. Experimental and theoretical study on the propagation characteristics of stress wave in filled jointed rock mass. *PLoS ONE*. 2021. Vol. 16 (9). N e0253392. DOI: 10.1371/journal.pone.0253392

29. Can Liu, Feifei Wang, Qingyang Ren et al. Field test of blasting vibration and adjacent slope stability under the influence of blasting vibration in mining. *Journal of Vibroengineering*. 2023. Vol. 25. Iss. 4, p. 713-728. DOI: 10.21595/jve.2022.22826

30. Rakishev B.R. Automated design and production of mass blasts in quarries. Almaty: Gylym, 2016, p. 340 (in Russian).

31. Masaev Yu.A., Masaev V.Yu., Drozdenko Yu.V., Aksenova O.Yu. Conditions of stress wave formation during blasting of borehole charges and their influence on rock fracture quality. *Bulletin of the Tomsk Polytechnic University. Geo Assets Engineering.* 2021. Vol. 332. N 11, p. 110-116 (in Russian). DOI: 10.18799/24131830/2021/11/3432

32. Zharikov S.N., Kutuev V.A. Construction of a nomogram for determining the parameters of DBW in the pit's contour zone. *News of the Tula State University. Sciences of Earth.* 2020. N 3, p. 161-171 (in Russian). DOI: 10.25635/r0915-0037-0746-z

33. Linghao Kong, Peng Yan, Wenbo Lu et al. Estimation of P-wave velocities based on pulse rise time in blasting vibration. *Measurement*. 2025. Vol. 258. Part A. N 119079. DOI: 10.1016/j.measurement.2025.119079

34. Botelho A.H., Dineva S., Ping Zhang, Nordlund E. Modification of seismic waves and particle velocity close to the excavation surface from mining-induced seismicity at Kiirunavaara Mine, Sweden. *Tunnelling and Underground Space Technology*. 2025. Vol. 165. N 106850. DOI: 10.1016/j.tust.2025.106850

***Authors*: Evgenii B. Shevkun,** *Doctor of Engineering Sciences, Professor* (*Pacific National University, Khabarovsk, Russia*), *https://orcid.org/0000-0001-5596-7700*, **Evgenii A. Shishkin,** *Candidate of Engineering Sciences, Associate Professor* (*Pacific National University, Khabarovsk, Russia*), *004655@togudv.ru*, *https://orcid.org/0000-0003-4387-0228*.

The authors declare no conflict of interests.